Experimental Measurements and Numerical Analysis of Al Deoxidation Equilibrium of Molten Fe–Cr–Ni Alloy

Hiroshi FUKAYA,[1]* Seika NAKAJIMA,[2] Jonah GAMUTAN,[3] Shigeru SUZUKI,[1] Koji KAJIKAWA,[1] Ken SAITO[4] and Takahiro MIKI[3]

1) Japan Steel Works M&E, Inc. Muroran Research Laboratory, 4, Chatsumachi, Muroran, 051-8505 Japan.
2) Graduate Student, Department of Metallurgy, Graduate School of Engineering, Tohoku University, Aoba-yama 6-6-02, Sendai, 980-8579 Japan.
3) Department of Metallurgy, Graduate School of Engineering, Tohoku University, Aoba-yama 6-6-02, Sendai, 980-8579 Japan.
4) JSW Joint Research Division, Graduate School of Engineering, Tohoku University, Aoba-yama 6-6-02, Sendai, 980-8579 Japan.

The aluminum deoxidation equilibrium in molten Fe-10 to 40mass%Cr-8mass%Ni and Fe-18mass%Cr-8 to 30mass%Ni alloys was experimentally determined at 1 873 K and 1 773 K to obtain the thermodynamic parameters at both temperatures, corresponding to the refining and casting processes, respectively. Thermodynamic analysis on Al deoxidation was carried out based on the sub-regular solution model using a Redlich–Kister type polynomial. Fe–Al, Ni–Al, Cr–Al and Fe–Cr–Ni interaction parameters were obtained from experimental results and a thermodynamic assessment. Using these parameters, the Al deoxidation equilibrium over the complete composition range of the Fe–Ni alloy and in more than 50mass%Fe of the Fe–Cr and Fe–Cr–Ni alloys can be calculated for the temperature ranges of both of the refining and casting processes.

KEY WORDS: quadratic formalism; thermodynamics; activity; excess free Gibbs energy; Redlich–Kister polynomial; aluminum deoxidation equilibrium; Fe–Cr–Ni alloy; sub-regular solution model: inclusion.

1. Introduction

Steels alloyed with chromium and nickel are some of the most popular alloy steels in the industry. Due to their excellent properties, Fe–Cr–Ni alloys are used in many applications as stainless steel, low-temperature steel, tool steel, heat-resistant steel, and so on.

To produce high quality steel, controlling the oxygen content in steel by deoxidation is important. Due to its strong affinity with oxygen and its availability, aluminum is commonly used as a deoxidizing agent during the steelmaking process. Therefore, several studies on the Al deoxidation equilibrium in the molten Fe–Ni and Fe–Cr binary alloys have been conducted.

So far, the Al deoxidation equilibrium in the Fe–Cr alloy system have been investigated by the following: Kishi *et al.*[1] in Fe-20mass%Cr at 1 873 K, Ohta & Suito[2] in Fe-8, 20, 40mass%Cr at 1 873 K, and Lee *et al.*[3] in Fe-16mass%Ni at 1 923 K by using levitation furnace. Ogasawara *et al.*[4] also investigated Al deoxidation equilibrium in Fe-10, 20, 30, 40mass%Cr with Al₂O₃ crucible at 1 873, 1 823 and 1 973 K.

In addition, the Al deoxidation equilibrium in the Fe–Ni alloy system have been studied by the following: Katsuki & Yamauchi[5] in Fe-36%Ni at 1 873 K, Cho & Suito[6] in Fe-30, 50, 70mass%Ni at 1 873 K, Li *et al.*[7] in Fe-36%Ni with a mullite crucible at 1 873 K, Ishii *et al.*[8] in Fe-50, 60, 70, 80, 90%Ni at 1 873, 1 923, 1 973 K and Ni at 1 823 to 1 973 K, Fujiwara *et al.*[9] in Fe-36mass%Ni at 1 973 K, Lee *et al.*[10] in Fe-36mass%Ni alloy at 1 773 K by using levitation furnace, Ohta & Suito[2] in Fe-10, 20, 40, 60mass%Ni at 1 873 K, Hayashi *et al.*[11] in Fe-20, 40mass%Ni at 1 873, 1 923 and 1 973 K, and Fukaya *et al.*[12] in Fe-36, 46mass%Ni at 1 773 and 1 873 K.

However, despite the importance of Fe–Cr–Ni alloy in the industry, the Al deoxidation equilibrium in Fe–Cr–Ni alloy has only been reported by Ohta & Suito.[2] They investigated the Al deoxidation equilibrium in Fe-18mass%Cr-8mass%Ni alloy at 1 873 K equilibrated with CaO–Al₂O₃ slag. Although Fe-18mass%Cr-8mass%Ni is the most common Fe–Cr–Ni alloy, it is not enough to obtain the thermodynamic parameters to calculate the Al deoxidation equilibrium in Fe–Cr–Ni alloys due to the wide composition range of practical Fe–Cr–Ni alloys. Furthermore, most

of these studies were carried out at temperature of 1 873 K or higher, because these studies were intended to describe and/or predict the reactions during the steel-refining process. However, to control the secondary inclusions that form due to cooling and solidification during the casting process, thermodynamic information around the liquidus temperature is also required. This issue has become much more important due to the increasing demand for ultra-high clean steels such as bearing steels, functional thin steel foils, and so on.

In this study, Al deoxidation equilibrium in molten Fe-10 to 40mass%Cr-8mass%Ni and Fe-18mass%Cr-8 to 30mass%Ni alloys was experimentally measured at 1 873 K and 1 773 K to describe the Al deoxidation equilibrium in Fe–Cr–Ni alloys. This is necessary to predict and/or control the Al deoxidation reaction at the refining and casting temperatures. Further, a thermodynamic assessment was carried out to obtain the interaction parameters based on the experimental results and reported studies. Using the parameters in this study, the Al deoxidation equilibrium over the complete composition range of Fe–Ni alloys and in the composition range of more than 50mass%Fe in Fe–Cr and Fe–Cr–Ni alloys can be calculated at the temperature ranges of both the refining and casting processes.

2. Experiment

In this study, the Al deoxidation experiments were carried out in Fe–10, 18, 30, 40mass%Cr–8mass%Ni and Fe–18mass%Cr–8, 20, 30mass%Ni alloys using an induction furnace at 1 773 K and 1 873 K. The experimental procedure is as follows. Reagent-grade electrolytic Fe (99.9% purity), Ni (99.9% purity) and Cr (99% purity) were used to prepare about 25 grams of alloy samples. High-purity Al (99.99% purity) or prepared Ni-5mass%Al alloy was used as the deoxidizer.

For enhanced reliability of the experimental results, equilibrated samples were obtained by melting twice in an Al_2O_3 crucible using a high-frequency induction furnace. Since the starting materials contain hundreds mass ppm of oxygen higher than the Al deoxidation equilibrium, Al_2O_3–Cr_2O_3 solid solution easily formed in the interface of Al_2O_3 crucible before deoxidation by Al or Ni–Al alloy. Once an Al_2O_3–Cr_2O_3 solid solution is formed, the complete reduction of Cr_2O_3 from the solid solution will be difficult. Therefore, in this study, the raw materials were first melted as a preliminary deoxidation step. After polishing the surface and cutting off the top part of the sample to remove the deoxidation products, the sample was melted again to obtain the equilibrated sample.

The melting procedure in the first and second melts were the same. Samples were placed in an Al_2O_3 crucible (OD: 21 mm, ID: 17 mm and Height: 100 mm) and heated in an Ar atmosphere (1.0 L/min) using a high-frequency induction heating furnace (MU-1700D, Sekisui Chemical Co., Ltd.) as shown in **Fig. 1**. Sample temperature was measured using a radiation thermometer (FTK-9, Japan Sensor Co., Ltd.). The emissivity of the radiation thermometer was calibrated by comparing the liquidus temperature of the Fe–Ni–Cr alloy. After the sample was completely melted at 1 873 K, Al or Ni–Al alloy was added to the molten sample through the injection pipe, and the sample was held at 1 873 K or
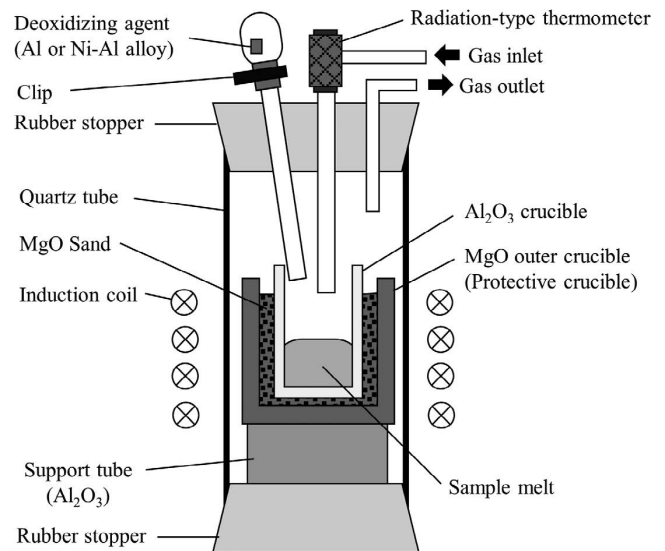
Fig. 1. Schematic diagram of the experimental setup.

1 773 K for another 20 minutes which was confirmed to be enough to reach equilibrium from the preliminary experiments. The sample melt was then quenched by cutting off the furnace power.

The chemical composition of the equilibrium samples was analyzed using the following techniques. After removing the shrinkage cavities from the equilibrium sample, the oxygen content was determined by an inert gas fusion technique (LECO-ONH836 Element Analyzer) using from about 0.3 to 1.0 g of samples. Due to the removal of the preliminary deoxidation products by double melting and the pinch effect of the induction furnace, the analyzed oxygen content is assumed to be the dissolved oxygen in the metal phase. Meanwhile, the Cr Ni and Al contents in the equilibrium samples were determined using an inductively coupled plasma emission spectrometer (ICPS-8100, Shimadzu Corp.). Approximately 0.3 to 1.0 g of the sample were dissolved in an aqua regia solution prepared by mixing 3-parts HCl to 1-part HNO_3. The Fe content of the samples was obtained as the remainder of the Cr, Ni, Al and O.

3. Experimental Results

The chemical compositions of the metal phase of the Fe–Cr–Ni alloys at 1 873 K and 1 773 K are shown in **Tables 1** and **2**, respectively. As mentioned before, in this study, the measured oxygen content was assumed to be the dissolved oxygen in the metal phase. The oxide composition at metal-crucible interface have been analyzed by SEM-EDS and it is confirmed to be Al_2O_3 (>98 mass%) in each experiments. So the activity of Al_2O_3 have been considered as unity in this paper. The Al–O equilibrium relationship in Fe-10 to 40mass%Cr-8mass%Ni alloy and Fe-18mass%Cr-8 to 30mass%Ni at 1 773 K and 1 873 K are shown in **Figs. 2** and **3**, respectively, along with the values previously reported by Ohta & Suito[2] (Fe-18mass%Cr-8mass%Ni at 1 873 K). Here, since Ohta & Suito measured the Al deoxidation by equilibrating with CaO–Al_2O_3 slag ($a_{Al_2O_3}$ = 0.33), the oxygen content was converted into the value of Al_2O_3 activity equal to unity. The solid and dashed lines shows the calculated equilibrium at 1 873 K and 1 773 K, respectively,

Table 1. Composition of Fe–Cr–Ni alloys at 1 873 K.

mass%Cr	mass%Ni	mass%Al	mass%O
9.67	7.76	0.00044	0.0239
9.55	8.04	0.0015	0.0324
9.72	7.87	0.0045	0.0058
9.63	7.94	0.0340	0.0020
9.58	8.23	0.129	0.0012
17.64	7.98	0.0015	0.0184
17.50	7.84	0.0021	0.0268
17.53	7.93	0.0383	0.0023
17.54	8.02	0.102	0.00087
17.55	7.99	0.226	0.0010
16.73	6.27	0.279	0.0014
17.74	20.43	0.0013	0.0372
17.84	20.45	0.0096	0.0084
17.69	20.33	0.047	0.0045
17.85	20.09	0.127	0.0037
17.85	30.41	0.0285	0.0129
17.62	29.99	0.0394	0.0070
18.20	29.03	0.0441	0.0093
18.02	30.35	0.0978	0.0033
29.92	8.15	0.0032	0.0154
29.65	7.93	0.0335	0.0103
29.72	8.11	0.139	0.0054
29.60	7.93	0.171	0.0044
29.69	8.08	0.179	0.0025
39.71	7.88	0.0023	0.0235
40.26	6.82	0.0032	0.0208
40.37	7.08	0.0048	0.0152
40.28	6.59	0.169	0.0018
39.88	6.56	0.249	0.0023

Table 2. Composition of Fe–Cr–Ni alloys at 1 773 K.

mass%Cr	mass%Ni	mass%Al	mass%O
9.72	7.83	0.0046	0.0032
9.53	7.75	0.0140	0.0024
9.67	7.83	0.0431	0.0010
9.88	8.09	0.0468	0.0010
9.54	7.76	0.0915	0.00084
9.16	7.08	0.1232	0.0011
17.55	7.10	0.00137	0.0122
17.67	7.89	0.0426	0.00066
17.48	8.20	0.0714	0.0011
17.51	7.49	0.131	0.00053
17.56	8.05	0.326	0.00061
17.67	20.24	0.00078	0.0324
17.94	20.21	0.0069	0.0030
17.83	20.29	0.0089	0.0054
17.86	20.26	0.0642	0.0021
17.59	20.10	0.234	0.0020
17.95	30.36	0.0102	0.0072
18.11	30.34	0.0244	0.0046
17.89	30.38	0.0291	0.0056
17.93	30.17	0.0460	0.0046
17.80	30.21	0.0567	0.0022
29.69	7.82	0.00033	0.0233
29.55	8.16	0.134	0.0020
29.53	8.04	0.189	0.0016
29.59	8.18	0.203	0.0014
29.46	7.87	0.248	0.0016
29.45	7.82	0.269	0.0025
29.83	8.19	0.283	0.0022
39.90	7.73	0.0017	0.0165
39.49	7.42	0.0339	0.0023
39.66	8.22	0.179	0.0018
39.72	8.10	0.192	0.00073
39.62	7.88	0.219	0.0013
39.45	7.96	0.291	0.0011

as discussed in Section 4. The Al deoxidation equilibrium product, $\log K'$ ($=\log([\text{mass\%Al}]^2[\text{mass\%O}]^3/a_{\text{Al}_2\text{O}_3})$), in Fe-Cr-8mass%Ni and Fe-18mass%Cr–Ni alloys are shown in **Figs. 4** and **5**. Here, the reported values of Fe-10mass%Ni (Ohta & Suito[2]) and Fe-20mass%Cr (Ohta & Suito,[2] Kishi[1] and Ogasawara[4]) are also plotted. As shown in Fig. 4, the $\log K'$ of Fe-Cr-8mass%Ni alloy increased with Cr content up to 30 mass%, beyond which value it decrease with increasing Cr contents. A similar tendency is observed in Fig. 5. The $\log K'$ of Fe-18mass%Cr–Ni alloy increased with Ni content up to 20mass%Ni and decreased with higher Ni content. These indicate that the Al deoxidation equilibrium in Fe–Cr–Ni alloy has a complex composition dependence which cannot be expressed in terms of a linear relationship.

4. Analysis

4.1. Thermodynamic Model for the Al Deoxidation Equilibrium

To describe the Al deoxidation equilibrium in Fe–Cr–Ni alloy, the sub-regular solution model with Redlich-Kister type polynomial[13,14] was used in this study, as was also applied to the Si deoxidation equilibrium by Miki & Hino.[15,16]

Wagner's type interaction parameter formalism (WIPF)[17] is the most popular method and commonly used in practical engineering. However, WIPF is, inherently, only available for dilute solutions. Although Kang et al.[18] described the Al deoxidation equilibrium of Fe with higher Al content by using secondary interaction parameters, there are many difficulties to applying WIPF to a wide composition range of high-alloy steels.

To describe the strong affinity between a deoxidizing element and oxygen, a modified quasi-chemical model (MQM)
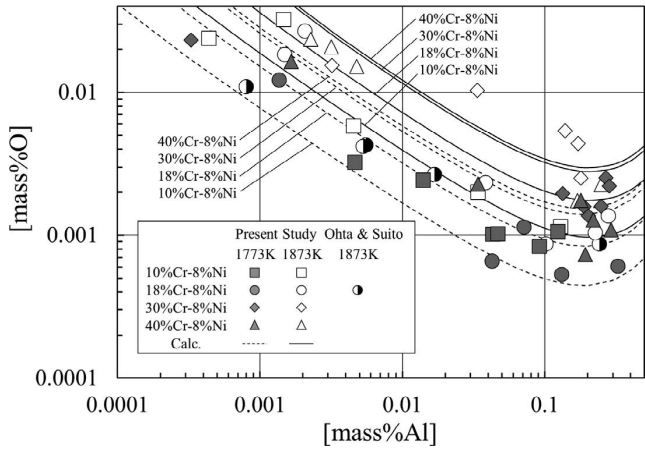
Fig. 2. Experimental results of Fe-10 to 40mass%Cr-8mass%Ni alloys.
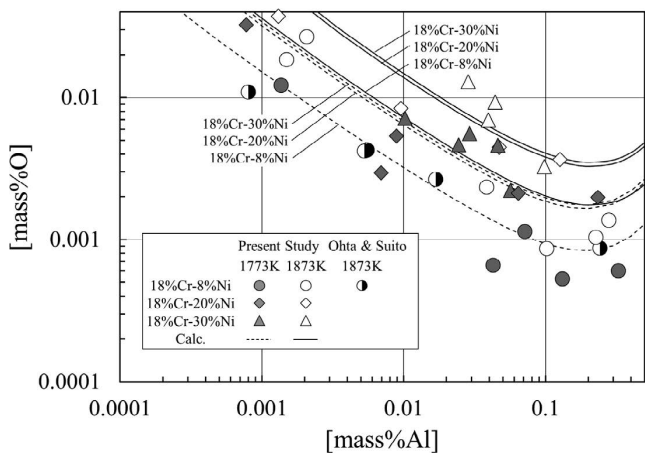
Fig. 3. Experimental results of Fe-18mass%Cr-8 to 30mass%Ni alloys.
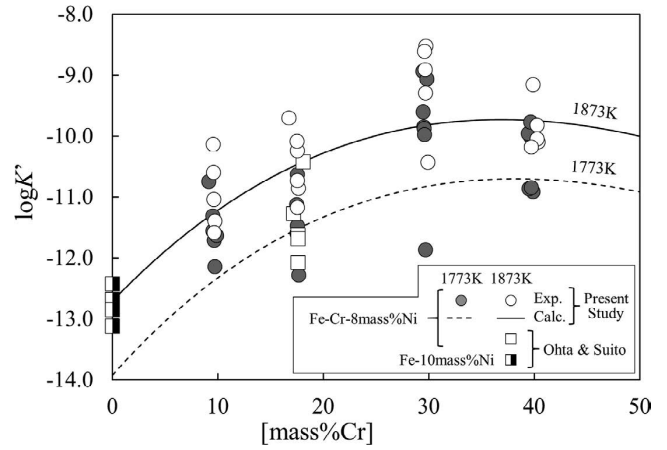
Fig. 4. $\log K'$ of Fe-Cr-8mass%Ni alloys at 1 773 K and 1 873 K.
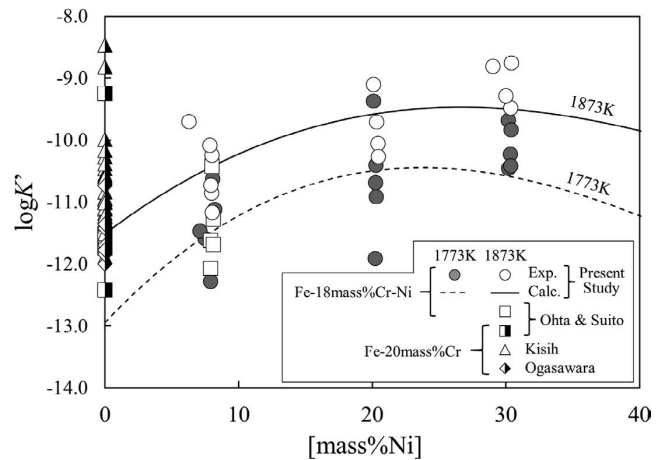
Fig. 5. $\log K'$ of Fe-18mass%Cr-Ni alloys at 1 773 K and 1 873 K.

has recently been developed. Paek *et al.*[19,20] have made it possible to describe the Al deoxidation equilibrium over the complete composition range of Fe–Al alloys. However, evaluation in multiple high-alloy systems, such as ternary systems, was not enough.

On the other hand, the sub-regular solution model is widely used in phase diagram calculation. Our research group applied this model to the Ti deoxidation of Fe,[21,22] Fe–Ni[23] and Fe–Cr and Fe–Cr–Ni[24] alloys, to the Mg deoxidation of Fe–Ni[25] and Fe–Cr–Ni[26] alloys and to the Al deoxidation of Fe–Ni alloy.[11,12] It was also confirmed that the sub-regular solution model is applicable to calculations of the deoxidation equilibriums of multiple high alloys.

The Al deoxidation equilibrium is described using the sub-regular solution model below. Using a Redlich-Kister type polynomial, the excess Gibbs free energy (ΔG^{ex}) is determined from Eq. (1).

$$\Delta G^{ex} = \sum X_i X_j \left(X_i - X_j \right)^n \Omega_{i-j}^n + \sum X_i X_j X_k \left(Y_i \Omega_{ijk}^i + Y_j \Omega_{ijk}^j + Y_k \Omega_{ijk}^k \right) \quad \text{........ (1)}$$

where X_i is the molar fraction of element i, Ω_{i-j}^n denotes the i-j binary interaction parameters, Ω_{ijk}^i denotes the i-j-k ternary interaction parameters and Y_i is the molar fraction of element i standardized into the i-j-k ternary system by Eqs. (2) to (4).

$$Y_i = X_i / \left(X_i + X_j + X_k \right) \quad \text{........................ (2)}$$

$$Y_j = X_j / \left(X_i + X_j + X_k \right) \quad \text{........................ (3)}$$

$$Y_k = X_k / \left(X_i + X_j + X_k \right) \quad \text{........................ (4)}$$

Using the excess Gibbs free energy change, the activity coefficients of Al and O are given by Eqs. (5) and (6), respectively.

$$RT \ln \gamma_{Al} = \Delta G^{ex} - X_{Cr} \frac{\partial \Delta G^{ex}}{\partial X_{Cr}} - X_{Ni} \frac{\partial \Delta G^{ex}}{\partial X_{Ni}} - X_O \frac{\partial \Delta G^{ex}}{\partial X_O}$$
$$+ \left(1 - X_{Al} \right) \frac{\partial \Delta G^{ex}}{\partial X_{Al}}$$
$$\text{......................... (5)}$$

$$RT \ln \gamma_O = \Delta G^{ex} - X_{Cr} \frac{\partial \Delta G^{ex}}{\partial X_{Cr}} - X_{Ni} \frac{\partial \Delta G^{ex}}{\partial X_{Ni}} - X_{Al} \frac{\partial \Delta G^{ex}}{\partial X_{Al}}$$
$$+ \left(1 - X_O \right) \frac{\partial \Delta G^{ex}}{\partial X_{Al}}$$
$$\text{......................... (6)}$$

For example, $RT\ln\gamma_{Al}$ of the Fe–Cr–Ni–Al–O system is described in Eq. (7). Here, ternary interaction terms except Fe–Cr–Ni and Fe–Ni–Al were omitted because there were

many combinations. $RT\ln\gamma_O$ is also obtained by exchanging Al for O in Eq. (7).

$$
\begin{aligned}
RT\ln\gamma_{Al} = & -\sum(n+1)X_{Fe}X_{Cr}\left(X_{Fe}-X_{Cr}\right)^n\Omega^n_{Fe-Cr} \\
& -\sum(n+1)X_{Fe}X_{Ni}\left(X_{Fe}-X_{Ni}\right)^n\Omega^n_{Fe-Ni} \\
& -\sum(n+1)X_{Cr}X_{Ni}\left(X_{Cr}-X_{Ni}\right)^n\Omega^n_{Cr-Ni} \\
& +\sum X_{Fe}\left(X_{Fe}-X_{Al}\right)^{n-1}\left\{X_{Fe}-(n+1)X_{Al}-(n+1)X_{Fe}X_{Al}+(n+1)X_{Al}^2\right\}\Omega^n_{Fe-Al} \\
& +\sum X_{Cr}\left(X_{Cr}-X_{Al}\right)^{n-1}\left\{X_{Cr}-(n+1)X_{Al}-(n+1)X_{Cr}X_{Al}+(n+1)X_{Al}^2\right\}\Omega^n_{Cr-Al} \\
& +\sum X_{Ni}\left(X_{Ni}-X_{Al}\right)^{n-1}\left\{X_{Ni}-(n+1)X_{Al}-(n+1)X_{Ni}X_{Al}+(n+1)X_{Al}^2\right\}\Omega^n_{Ni-Al} \\
& -\sum(n+1)X_{Fe}X_O\left(X_{Fe}-X_O\right)^n\Omega^n_{Fe-O} \\
& -\sum(n+1)X_{Cr}X_O\left(X_{Cr}-X_O\right)^n\Omega^n_{Cr-O} \\
& -\sum(n+1)X_{Fe}X_O\left(X_{Fe}-X_O\right)^n\Omega^n_{Ni-O} \\
& -\sum X_O\left(X_{Al}-X_O\right)^{n-1}\left\{X_O-(n+1)X_{Al}-(n+1)X_{Al}X_O+(n+1)X_{Al}^2\right\}\Omega^n_{Al-O} \\
& -2X_{Fe}X_{Cr}X_{Ni}\left(Y_{Fe}\Omega^{Fe}_{FeCrNi}+Y_{Cr}\Omega^{Cr}_{FeCrNi}+Y_{Ni}\Omega^{Ni}_{FeCrNi}\right) \\
& +X_{Fe}X_{Ni}\left(1-Y_{Al}-2X_{Al}\right)\left(Y_{Fe}\Omega^{Fe}_{FeNiAl}+Y_{Ni}\Omega^{Ni}_{FeNiAl}+Y_{Al}\Omega^{Al}_{FeNiAl}\right) \\
& +X_{Fe}X_{Ni}Y_{Al}\Omega^{Al}_{AlFeNi}
\end{aligned}
$$
.... (7)

Miki & Hino[15,16] applied this model to the calculation of the deoxidation equilibrium by taking the standard state of oxygen as the dissolved oxygen equilibrating with 1 atm of O_2 gas. In this condition, the dissolution reaction of oxygen gas is expressed in Eq. (8) and its Gibbs free energy change is equal to zero (Eq. (9)).

$$2\underline{O}=O_2(g) \quad\quad\text{................................ (8)}$$

$$\Delta G^\circ = -RT\ln\frac{P_{O_2}}{a_O^2}=0 \ \left(\because P_{O_2}=a_O^2\right)\text{............. (9)}$$

The Al deoxidation reaction and its Gibbs free energy change can be expressed as Eq. (10). Since Eq. (9) is equal to zero, Eq. (10) is equal to the Gibbs free energy of Al_2O_3 formation ($\Delta G^\circ_{f,Al_2O_3}$,[11] Eq. (11)) and Eq. (12) was obtained. By introducing the activity coefficient ($RT\ln\gamma_{Al}$, $RT\ln\gamma_O$) described using the excess Gibbs free energy (Eqs. (5) and (6)) into Eq. (12), the Al deoxidation equilibrium is calculated using the molar fraction and interaction parameters. In this study, a thermodynamic assessment was carried out based on this equation.

$$2\underline{Al}+3\underline{O}=Al_2O_3 : \Delta G^\circ=RT\ln\frac{a_{Al}^2 a_O^3}{a_{Al_2O_3}} \text{........ (10)}$$
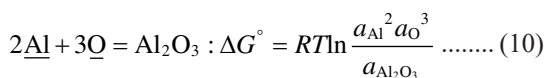
$$
\begin{aligned}
2Al(l)+\frac{3}{2}O_2(g)=Al_2O_3(s) &: \Delta G^\circ_{Al_2O_3} \\
&= -1\,682\,300+324.15T^{27)}
\end{aligned}
\text{.... (11)}
$$

$$
\begin{aligned}
\Delta G^\circ_{Al_2O_3} &= RT\ln\frac{a_{Al}^2 a_O^3}{a_{Al_2O_3}} \\
&= RT\ln X_{Al}^2 X_O^3 + 2RT\ln\gamma_{Al}+3RT\ln\gamma_O - RT\ln a_{Al_2O_3}
\end{aligned}
$$
.... (12)

4.2. Re-assessment in the Fe–Ni–Al–O System

The interaction parameters for the Fe–Ni–Al–O system were determined in a previous study.[12] Although the Al deoxidation equilibrium over the complete composition range of Fe–Ni alloys was calculated using these parameters, the Ni–Al interaction parameters are inconsistent in
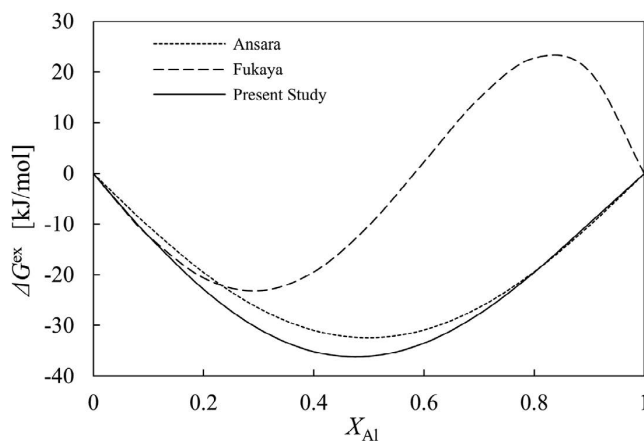
Fig. 6. Excess free energy of the Ni–Al system at 1 873 K.
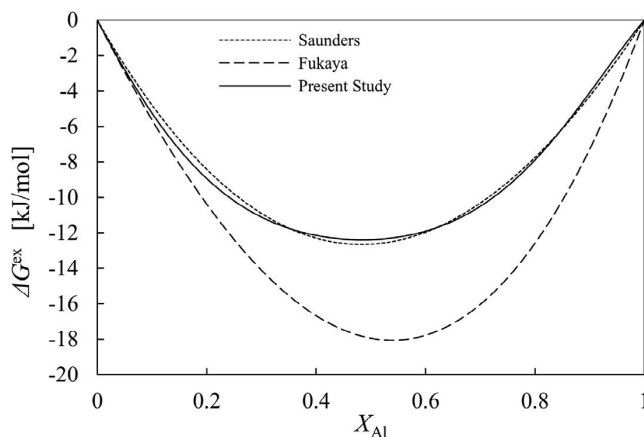
Fig. 7. Excess free energy of the Fe–Al system at 1 873 K.

the higher Al range. **Figure 6** shows the excess Gibbs free energy of the Ni–Al binary system (ΔG^{ex}) calculated from the Ni–Al interaction parameters. Using our previously parameters, ΔG^{ex} changes from a negative value to a positive value in the higher Al range. It also deviated greatly from Ansara et al.[28] which was well used in the phase diagram. This is because, in the previous study, the Ni–Al interaction was determined by fitting the large composition dependence of $\log K'$ of Fe–Ni alloy without ternary interaction terms. Although it will not be a problem for the Al deoxidation of the Fe–Ni system, it can cause serious errors in other systems. Therefore, we reassessed the Al deoxidation of Fe–Ni alloy.

In the previous study,[12] the interaction between solvent elements (Fe–Ni[29]) were taken from the values that are commonly used in the field of phase diagrams. On the other hand, the interactions between solvents and solutes (Ni–Al,[12] Fe–Al,[12] Fe–O,[16] Ni–O[16]) was determined from the deoxidation equilibrium, the Gibbs free energy change of the dissolution reaction and/or Wagner's interaction parameters. This means that the later value was obtained only from the dilute compositions. Therefore, as shown in **Fig. 7**, ΔG^{ex} of the Fe–Al system calculated from the Fe–Al interaction determined in our previous study[12] deviated from that of the Saunders's interaction[30] which was determined from a wide composition rage of the Fe–Al system and is commonly used in the phase diagram. So, the Fe–Al interaction parameter (Eqs. (13)–(17)) in this study was newly determined by

fitting the dilute Al area with the value of Fukaya[12] and the higher Al area with the value of Saunders.[30]

$$\Omega^0_{Fe-Al} = -60\,072 + 10.43\,T\,\left[J\,/\,mol\right] \dots\dots (13)$$

$$\Omega^1_{Fe-Al} = -42\,886 - 23.03\,T\,\left[J\,/\,mol\right] \dots\dots (14)$$

$$\Omega^2_{Fe-Al} = -336\,944 + 172.0\,T\,\left[J\,/\,mol\right] \dots\dots (15)$$

$$\Omega^3_{Fe-Al} = -246\,795 + 126.8\,T\,\left[J\,/\,mol\right] \dots\dots (16)$$

$$\Omega^4_{Fe-Al} = 368\,534 - 187.4\,T\,\left[J\,/\,mol\right] \dots\dots (17)$$

By introducing higher order Al–O interaction parameters, the thermodynamic model of this study can also be used to calculate the deoxidation equilibrium over the complete composition range of the Fe–Al system. However, except for the Fe–Al–O system, the Al deoxidation equilibrium with such higher Al content was not reported. Even though it can be used to calculate the higher Al range in the Fe–Cr–Ni alloy, the reliability of the calculation cannot be evaluated. Therefore, in this study, the previous Al–O interaction[12] consisting of only the 1st order parameter was used although the calculation validity of this parameter was limited to less than 0.5mass%Al. Considering practical Fe–Cr–Ni alloy compositions, excepting high Al special steels, this composition range is enough to apply in the actual engineering situations.

Re-assessment of the Al deoxidation in molten Fe–Ni alloy was carried out with the Fe–Ni–Al ternary interaction parameters of Zhang[31] and the newly determined Fe–Al interaction parameters. The Ni–Al interaction parameter (Eqs. (18)–(20)) was determined from the composition dependence of $\log K'$ for the Al deoxidation equilibrium in Fe–Ni alloys. The details of how that was determined are described in a previous paper.[12] The calculated $\log K'$ and experimental data of the Al deoxidation equilibrium in Fe–Ni alloys[2,5–12] are shown in **Fig. 8**. Both calculated lines agree well with the reported values. The excess Gibbs free energy of Ni–Al system calculated using the newly determined Ni–Al interaction parameters are also shown in Fig.
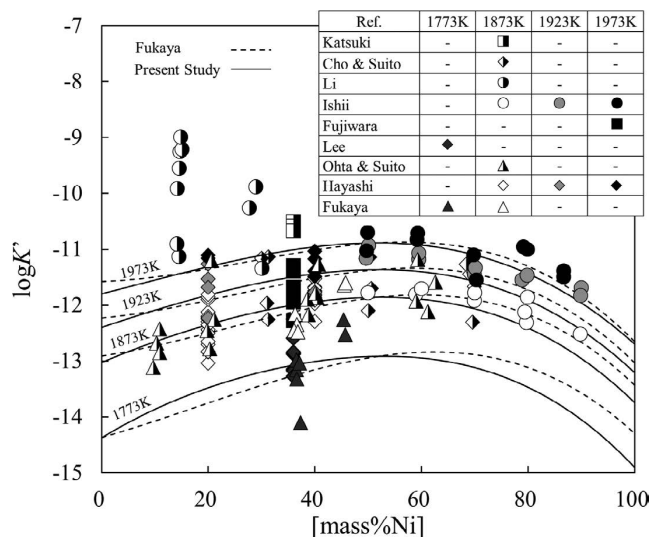
6. Using the new Ni–Al interaction values, excess Gibbs free energy values similar to those of Ansara *et al.*[28] were obtained. This indicates that the re-assessed parameters are much more reliable than the previous value.

$$\Omega^0_{Ni-Al} = -364\,875 + 117.7\,T\,\left[J\,/\,mol\right] \dots\dots (18)$$

$$\Omega^1_{Ni-Al} = -90\,760 + 39.16\,T\,\left[J\,/\,mol\right] \dots\dots (19)$$

$$\Omega^2_{Ni-Al} = 87\,230 - 28.91\,T\,\left[J\,/\,mol\right] \dots\dots (20)$$

4.3. Assessment in the Fe–Cr–Al–O System

Thermodynamic analysis in the Fe–Cr system was carried out from the reported Al deoxidation equilibrium of the Fe–Cr alloys.[1–4] When the Al and O contents are small enough and the activity of Al_2O_3 is unity, the Al deoxidation equilibrium of Fe–Cr alloys is simply expressed as in Eq. (21).

$$\Delta G^\circ_{Al_2O_3} = RT\ln X_{Al}^2 X_O^3 + 2RT\ln\gamma_{Al} + 3RT\ln\gamma_O$$
$$= RT\ln X_{Al}^2 X_O^3 - 5\sum(n+1)X_{Fe}X_{Cr}\left(X_{Fe}-X_{Cr}\right)^n\Omega^n_{Fe-Cr}$$
$$+2\sum X_{Fe}^{n+1}\Omega^n_{Fe-Al} + 2\sum X_{Cr}^{n+1}\Omega^n_{Cr-Al}$$
$$+3\sum X_{Fe}^{n+1}\Omega^n_{Fe-O} + 3\sum X_{Cr}^{n+1}\Omega^n_{Cr-O}$$
$$\dots\dots (21)$$

Here, as the Fe–Al and Fe–O interactions used the same parameters as the previous Fe–Ni re-assessment and reported values for Fe–Cr[29] and Cr–O[24] were used, all interaction terms except Cr–Al were obtained. By transferring all terms of Eq. (21) except the Cr–Al interaction, and defining F_{Cr-Al}, Eq. (22) was obtained.

$$F_{Cr-Al} = \Delta G^\circ_{Al_2O_3} - RT\ln X_{Al}^2 X_O^3$$
$$+5\sum(n+1)X_{Fe}X_{Cr}\left(X_{Fe}-X_{Cr}\right)^n\Omega^n_{Fe-Cr}$$
$$-2\sum X_{Fe}^{n+1}\Omega^n_{Fe-Al} - 3\sum X_{Fe}^{n+1}\Omega^n_{Fe-O} - 3\sum X_{Cr}^{n+1}\Omega^n_{Cr-O}$$
$$= 2\sum X_{Cr}^{n+1}\Omega^n_{Cr-Al}$$
$$\dots\dots (22)$$

Here F_{Cr-Al} is simply expressed as an n order function of X_{Cr}. F_{Cr-Al} calculated from the reported Al deoxidation equilibrium is shown in **Fig. 9**. In this figure, the solid lines are the fitting curves with the second order Cr–Al interaction (Eqs. (23) and (24)).

Ref.	1773K	1873K	1923K	1973K
Katsuki	-	▣	-	-
Cho & Suito	-	◇	-	-
Li	-	◐	-	-
Ishii	-	○	●	●
Fujiwara	-	-	-	■
Lee	◆	-	-	-
Ohta & Suito	-	▲	-	-
Hayashi	-	◇	◆	◆
Fukaya	▲	△	-	-

Fig. 8. Calculated and reported $\log K'$ of the Al deoxidation equilibrium of the Fe–Ni system.
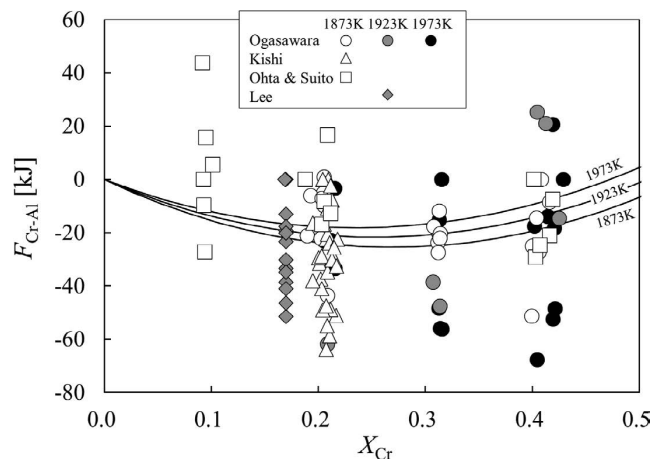
Fig. 9. Relation between F_{Cr-Al} and X_{Cr}.

$$\Omega^0_{Cr-Al} = 2\,548\,740 - 179.0\,T\ [\mathrm{J}\,/\,\mathrm{mol}] \ \dots\dots\ (23)$$

$$\Omega^1_{Cr-Al} = -87\,250 + 133.2\,T\ [\mathrm{J}\,/\,\mathrm{mol}] \ \dots\dots\ (24)$$

Since the reported Al deoxidation equilibrium of Fe–Cr alloys is limited with less than 40mass%Cr, the tendency of the F_{Cr-A} for the whole Fe–Cr system is not clear. If F_{Cr-Al} is drastically changed to the higher Cr range, higher order interaction will be required. The calculated and reported $\log K'$ of the Al deoxidation equilibrium in Fe–Cr alloys are shown in **Fig. 10**. The calculated lines with the newly obtained Cr–Al interaction were found to be in good agreement with the reported values. This indicates that the second order interaction is enough for the compositions with less than 40mass%Cr.

4.4. Assessment in the Fe–Ni–Cr–Al–O System

Since the Al deoxidation equilibriums in the Fe–Ni and Fe–Cr binary systems were determined, that of the Fe–Cr–Ni system can also be calculated using the Cr–Ni[29] and Fe–Cr–Ni[32] ternary interaction parameters.

The relationship between the calculated and experimental $\log K'$ of the Al deoxidation equilibrium in Fe–Cr–Ni alloys at 1 873 K for the same Fe molar fraction (about $X_{Fe}=0.6$) and equivalent molar fraction of Cr ($X_{Cr}/(X_{Cr}+X_{Ni})$) is shown

in **Fig. 11**. In this figure, both ends of the horizontal axis shows the values for the Fe–Cr and Fe–Ni binary systems which were already determined. The experimental values in
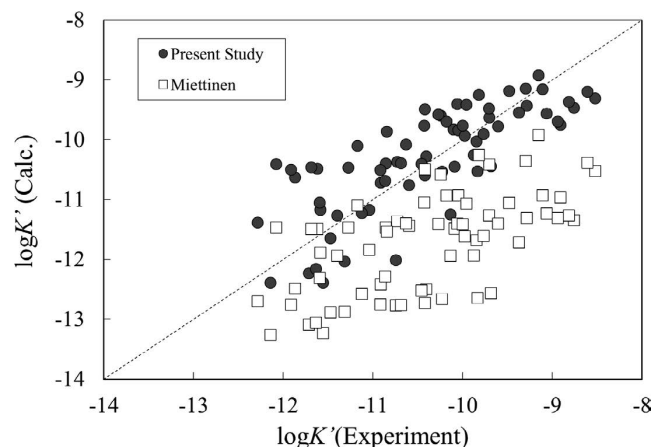
Fig. 12. Comparison between the calculated $\log K'$ of the Al deoxidation equilibrium of the Fe–Ni–Cr system with different Fe–Cr–Ni ternary interaction parameter.
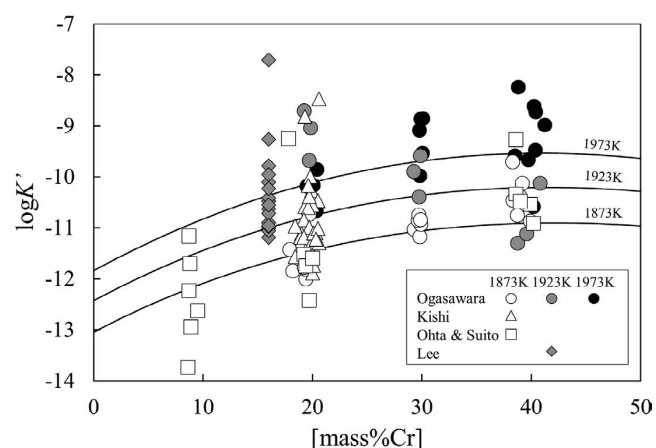
Fig. 10. Calculated and reported $\log K'$ of the Al deoxidation equilibrium of the Fe–Cr system.
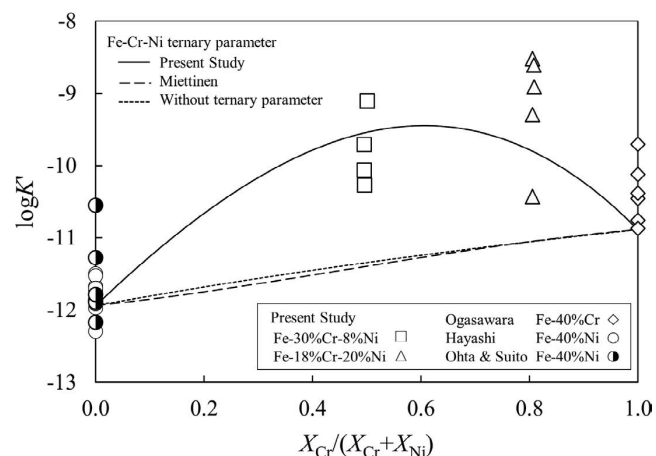
Fig. 11. Calculated and reported $\log K'$ of the Al deoxidation equilibrium of the Fe–Ni–Cr system ($X_{Fe}=0.60$) at 1 873 K.

Table 3. List of interaction parameters used in this study.

	Value [J/mol]		Ref.
Ω^0_{Fe-Cr}	−17 737	+7.997 T	(29)
Ω^1_{Fe-Cr}	1 331		
Ω^0_{Fe-Ni}	−16 911	+5.162 T	(29)
Ω^1_{Fe-Ni}	10 180	−4.147 T	
Ω^0_{Cr-Ni}	318	−7.33 T	(29)
Ω^1_{Cr-Ni}	16 941	−6.37 T	
Ω^0_{Fe-Al}	−69 072	+10.43 T	
Ω^1_{Fe-Al}	42 886	−24.03 T	
Ω^2_{Fe-Al}	−336 944	+172.0 T	Present Study
Ω^3_{Fe-Al}	−246 795	+126.8 T	
Ω^4_{Fe-Al}	368 534	−187.4 T	
Ω^0_{Cr-Al}	258 740	−179.0 T	Present Study
Ω^1_{Cr-Al}	−87 250	+133.2 T	
Ω^0_{Ni-Al}	−364 875	+117.7 T	
Ω^1_{Ni-Al}	−90 760	+39.16 T	Present Study
Ω^2_{Ni-Al}	87 230	−28.91 T	
Ω^0_{Fe-O}	−415 400	+142.4 T	(16)
Ω^1_{Fe-O}	298 300	−117.8 T	
Ω^0_{Cr-O}	−52 870	−24 T	(24)
Ω^1_{Cr-O}	−498 200	+235 T	
Ω^0_{Ni-O}	−106 500	+44.80 T	(16)
Ω^1_{Ni-O}	35 500	−15.920 T	
Ω^0_{Al-O}	−5 626 500	+1 635 T	(12)
Ω^{Fe}_{FeCrNi}	2 623 669	−1 171 T	
Ω^{Cr}_{FeCrNi}	2 748 122	−1 391 T	Present Study
Ω^{Ni}_{FeCrNi}	−4 365 536	+2 277 T	
Ω^{Fe}_{FeNiAl}	57 195		
Ω^{Ni}_{FeNiAl}	−8 441		(31)
Ω^{Al}_{FeNiAl}	−62 066	+11.763 T	
ΔG°_{Al2O3}	−1 682 300	+324.15 T	(27)

Fe-30%massCr-8mass%Ni and Fe-18mass%Cr-20mass%Ni from the present study, Fe-40mass%Cr from Ogasawara,[4] Fe-40%mass%Ni from Ohta & Suito[2] and Hayashi[11] were also plotted. As shown in Fig. 11, log$K$' of the Fe–Cr–Ni alloy was an upward convex curve and the value is larger than that of the Fe–Ni and Fe–Cr systems. It cannot be expressed by the calculation without the Fe–Cr–Ni ternary parameter nor with the reported ternary parameter.[32] Although it can be modified by introducing the Cr–Ni–Al and/or Cr–Ni–O ternary interaction terms as a fitting parameter, the interaction becomes too big at the higher Ni and Cr contents. It might be unrealistic. Therefore, in this study, the Fe–Cr–Ni interaction parameter was modified. To fit the experimental data for the Fe–Cr–Ni alloy of the present study as well as that of Ohta & Suito,[2] a Fe–Cr–Ni ternary interaction parameter was determined as in Eqs. (25)–(27). In **Fig. 12**, the calculated log$K$' was compared with the experimental values. It is clear that calculation was improved by using the optimized parameter in this study.

Fig. 13. Calculated log$K$' of the Al deoxidation equilibrium of the Fe–Ni system on the phase diagram.

Fig. 14. Calculated log$K$' of the Al deoxidation equilibrium of the Fe–Cr–Ni system at 1 873 K.

$$\Omega^{\mathrm{Fe}}_{\mathrm{FeCrNi}} = 2\,623\,669 - 1171\,T\ [\mathrm{J/mol}] \quad\text{(25)}$$

$$\Omega^{\mathrm{Cr}}_{\mathrm{FeCrNi}} = 2\,748\,122 - 1\,391\,T\ [\mathrm{J/mol}] \quad\text{(26)}$$

$$\Omega^{\mathrm{Ni}}_{\mathrm{FeCrNi}} = -4\,365\,536 + 2\,277\,T\ [\mathrm{J/mol}] \quad\text{(27)}$$

However, it cannot evaluate the reliability of the Fe–Cr–Ni parameter reported by Miettinen.[32] The values and temperature dependence of the newly determined Fe–Cr–Ni parameter were too big. It might involve other ternary parameters and/or higher order interactions which were not considered in this study. Therefore, this parameter can be used only for the Al deoxidation equilibrium in Fe–Cr–Ni alloys and can cause errors when used for other purposes or in other alloy systems.

Although the parameter usage is limited, the Al deoxidation equilibrium of iron rich Fe–Cr–Ni alloys can be calculated precisely. The deoxidation equation is expressed in Eq. (28) with the interaction parameters used in this study. All parameters are shown in **Table 3**.

$$
\begin{aligned}
\Delta G^{\circ}_{f,\mathrm{Al_2O_3}} =\ & RT\ln X_{\mathrm{Al}}^2 X_{\mathrm{O}}^3 - RT\ln a_{\mathrm{Al_2O_3}} \\
& -5X_{\mathrm{Fe}}X_{\mathrm{Fe}}\Omega^0_{\mathrm{Fe-Cr}} - 10X_{\mathrm{Fe}}X_{\mathrm{Cr}}\left(X_{\mathrm{Fe}}-X_{\mathrm{Cr}}\right)\Omega^1_{\mathrm{Fe-Cr}} \\
& -5X_{\mathrm{Fe}}X_{\mathrm{Fe}}\Omega^0_{\mathrm{Fe-Ni}} - 10X_{\mathrm{Fe}}X_{\mathrm{Ni}}\left(X_{\mathrm{Fe}}-X_{\mathrm{Ni}}\right)\Omega^1_{\mathrm{Fe-Ni}} \\
& -5X_{\mathrm{Cr}}X_{\mathrm{Cr}}\Omega^0_{\mathrm{Cr-Ni}} - 10X_{\mathrm{Cr}}X_{\mathrm{Ni}}\left(X_{\mathrm{Cr}}-X_{\mathrm{Ni}}\right)\Omega^1_{\mathrm{Cr-Ni}} \\
& +X_{\mathrm{Fe}}\left(3-5X_{\mathrm{O}}\right)\Omega^0_{\mathrm{Fe-O}} \\
& +X_{\mathrm{Fe}}\left(3X_{\mathrm{Fe}}-6X_{\mathrm{O}}-10X_{\mathrm{Fe}}X_{\mathrm{O}}+10X_{\mathrm{O}}^2\right)\Omega^1_{\mathrm{Fe-O}} \\
& +X_{\mathrm{Cr}}\left(3-5X_{\mathrm{O}}\right)\Omega^0_{\mathrm{Cr-O}} \\
& +X_{\mathrm{Cr}}\left(3X_{\mathrm{Cr}}-6X_{\mathrm{O}}-10X_{\mathrm{Cr}}X_{\mathrm{O}}+10X_{\mathrm{O}}^2\right)\Omega^1_{\mathrm{Cr-O}} \\
& +X_{\mathrm{Ni}}\left(3-5X_{\mathrm{O}}\right)\Omega^0_{\mathrm{Ni-O}} \\
& +X_{\mathrm{Ni}}\left(3X_{\mathrm{Ni}}-6X_{\mathrm{O}}-10X_{\mathrm{Ni}}X_{\mathrm{O}}+10X_{\mathrm{O}}^2\right)\Omega^1_{\mathrm{Ni-O}} \\
& +X_{\mathrm{Fe}}\left(2-5X_{\mathrm{Al}}\right)\Omega^0_{\mathrm{Fe-Al}} \\
& +X_{\mathrm{Fe}}\left(2X_{\mathrm{Fe}}-4X_{\mathrm{Al}}-10X_{\mathrm{Fe}}X_{\mathrm{Al}}+10X_{\mathrm{Al}}^2\right)\Omega^1_{\mathrm{Fe-Al}} \\
& +X_{\mathrm{Fe}}\left(X_{\mathrm{Fe}}-X_{\mathrm{Al}}\right)\left(2X_{\mathrm{Fe}}-6X_{\mathrm{Al}}-15X_{\mathrm{Fe}}X_{\mathrm{Al}}+15X_{\mathrm{Al}}^2\right)\Omega^2_{\mathrm{Fe-Al}} \\
& +X_{\mathrm{Fe}}\left(X_{\mathrm{Fe}}-X_{\mathrm{Al}}\right)^2\left(2X_{\mathrm{Fe}}-8X_{\mathrm{Al}}-20X_{\mathrm{Fe}}X_{\mathrm{Al}}+20X_{\mathrm{Al}}^2\right)\Omega^3_{\mathrm{Fe-Al}} \\
& +X_{\mathrm{Fe}}\left(X_{\mathrm{Fe}}-X_{\mathrm{Al}}\right)^3\left(2X_{\mathrm{Fe}}-10X_{\mathrm{Al}}-25X_{\mathrm{Fe}}X_{\mathrm{Al}}+25X_{\mathrm{Al}}^2\right)\Omega^4_{\mathrm{Fe-Al}} \\
& +X_{\mathrm{Cr}}\left(2-5X_{\mathrm{Al}}\right)\Omega^0_{\mathrm{Cr-Al}} \\
& +X_{\mathrm{Cr}}\left(2X_{\mathrm{Cr}}-4X_{\mathrm{Al}}-10X_{\mathrm{Cr}}X_{\mathrm{Al}}+10X_{\mathrm{Al}}^2\right)\Omega^1_{\mathrm{Cr-Al}} \\
& +X_{\mathrm{Ni}}\left(2-5X_{\mathrm{Al}}\right)\Omega^0_{\mathrm{Ni-Al}} \\
& +X_{\mathrm{Ni}}\left(2X_{\mathrm{Ni}}-4X_{\mathrm{Al}}-10X_{\mathrm{Ni}}X_{\mathrm{Al}}+10X_{\mathrm{Al}}^2\right)\Omega^1_{\mathrm{Ni-Al}} \\
& +X_{\mathrm{Ni}}\left(X_{\mathrm{Ni}}-X_{\mathrm{Al}}\right)\left(2X_{\mathrm{Ni}}-6X_{\mathrm{Al}}-15X_{\mathrm{Ni}}X_{\mathrm{Al}}+15X_{\mathrm{Al}}^2\right)\Omega^2_{\mathrm{Ni-Al}} \\
& +\left(3X_{\mathrm{Al}}+2X_{\mathrm{O}}-5X_{\mathrm{Al}}X_{\mathrm{O}}\right)\Omega^1_{\mathrm{Al-O}} \\
& +X_{\mathrm{Fe}}X_{\mathrm{Ni}}\left(2-2Y_{\mathrm{Al}}-10X_{\mathrm{Al}}\right)\left(Y_{\mathrm{Al}}\Omega^{\mathrm{Al}}_{\mathrm{AlFeNi}}+Y_{\mathrm{Fe}}\Omega^{\mathrm{Fe}}_{\mathrm{AlFeNi}}+Y_{\mathrm{Ni}}\Omega^{\mathrm{Ni}}_{\mathrm{AlFeNi}}\right) \\
& +2Y_{\mathrm{Al}}X_{\mathrm{Fe}}X_{\mathrm{Ni}}\Omega^{\mathrm{Al}}_{\mathrm{AlFeNi}} \\
& -10X_{\mathrm{Fe}}X_{\mathrm{Cr}}X_{\mathrm{Ni}}\left(Y_{\mathrm{Fe}}\Omega^{\mathrm{Fe}}_{\mathrm{FeCrNi}}+Y_{\mathrm{Cr}}\Omega^{\mathrm{Cr}}_{\mathrm{FeCrNi}}++Y_{\mathrm{Ni}}\Omega^{\mathrm{Ni}}_{\mathrm{FeCrNi}}\right)
\end{aligned}
$$

$$\text{.................................... (28)}$$

Since these parameters were optimized from the deoxidation equilibrium between 1 773 and 1 973 K, it might also be available at the liquidus temperature. Using this
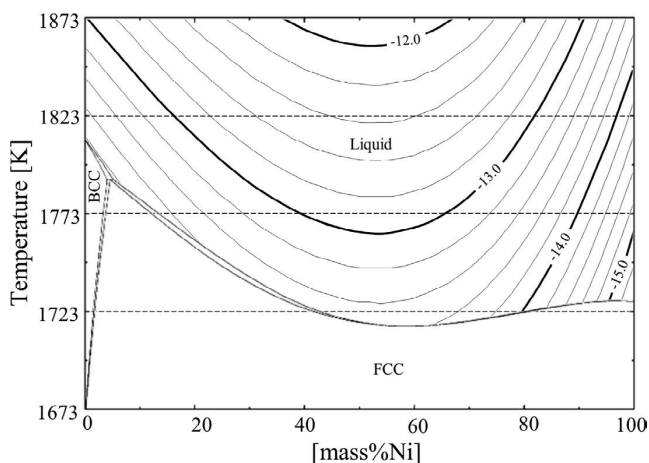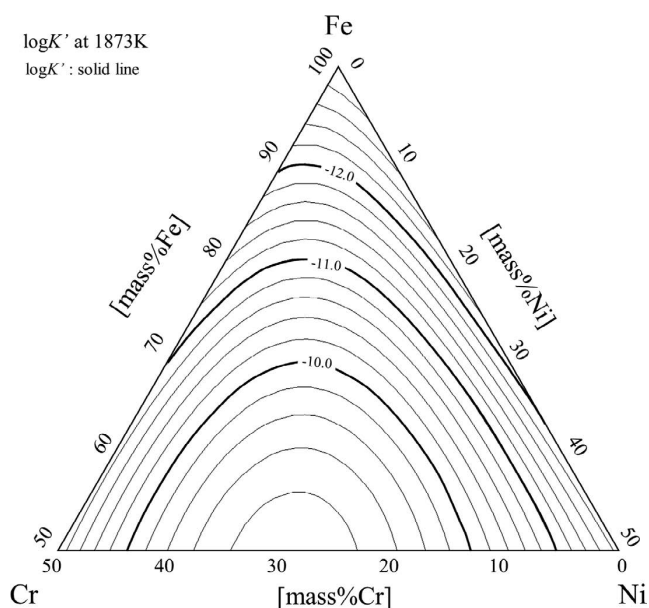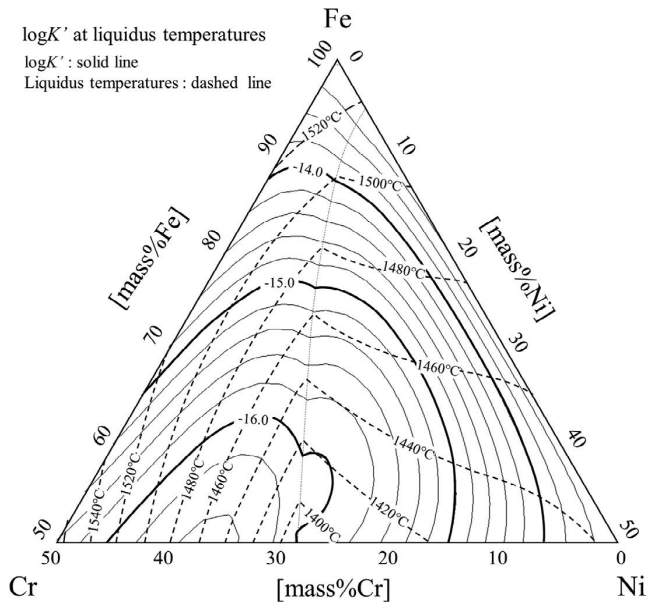
Fig. 15. Calculated log$K$' of the Al deoxidation equilibrium of the Fe–Cr–Ni system at liquidus temperatures.

equation and the determined parameters, the Al deoxidation equilibrium was calculated for the complete composition range of Fe–Ni alloys and Fe–Cr–Ni alloy with more than 50mass%Fe at the steel refining and casting temperatures. For example, the calculated log$K$'(Al=0.01 mass%) described on the Fe–Ni phase diagram is shown in **Fig. 13**. Also, the log$K$' in Fe–Cr–Ni alloys at 1 873 K and at the liquidus temperatures are shown in **Figs. 14** and **15**, respectively. In those figures, the phase diagrams and liquidus temperatures were calculated using FactSage.[33] This information is of significant help for the prediction and/or control of secondary inclusions in the practical steelmaking operations.

5. Conclusion

The Al deoxidation equilibrium in molten Fe–Cr–Ni alloy was experimentally determined at 1 773 and 1 873 K. A thermodynamic assessment based on the sub-regular solution model using a Redlich-Kister type polynomial was carried out. In the Fe–Ni–Al–O, Fe–Cr–Al–O and Fe–Cr–Ni–Al–O systems, Fe–Al, Ni–Al, Cr–Al and Fe–Cr–Ni interaction parameters were newly determined. Using these parameters, the Al deoxidation equilibrium in the complete composition range of Fe–Ni alloys and the Fe rich Fe–Cr–Ni alloys (>50mass%Fe) can be described at the liquidus temperature and to 1 973 K with lower Al composition (<0.5mass%Al).

REFERENCES

1) M. Kishi, R. Inoue and H. Suito: *ISIJ Int.*, **34** (1994), 859.
2) H. Ohta and H. Suito: *ISIJ Int.*, **43** (2003), 1301.
3) S. B. Lee, J. H. Choi, H. G. Lee, P. C. H. Rhee and S. M. Jung: *Metall. Mater. Trans. B*, **36** (2005), 414.
4) Y. Ogasawara and T. Miki: *CAMP-ISIJ*, **23** (2010), 925 (in Japanese), CD-ROM.
5) J. Katsuki and T. Yamauchi: *CAMP-ISIJ*, **7** (1994), 1076 (in Japanese).
6) S. W. Cho and H. Suito: *Steel Res.*, **66** (1995), 237.
7) G. Li, R. Inoue and H. Suito: *Steel Res.*, **67** (1996), 528.
8) F. Ishii, S. Ban-ya and M. Hino: *ISIJ Int.*, **36** (1996), 25.
9) H. Fujiwara, A. Hattori and E. Ichise: *Tetsu-to-Hagané*, **85** (1999), 201 (in Japanese).
10) S. B. Lee, S. M. Jung, H. G. Lee and C. H. Rhee: *ISIJ Int.*, **42** (2002), 679.
11) A. Hayashi, T. Uenishi, H. Kandori, T. Miki and M. Hino: *ISIJ Int.*, **48** (2008), 1533.
12) H. Fukaya, K. Kajikawa, A. Malfliet, B. Blanpain and M. Guo: *Metall. Mater. Trans. B*, **49** (2018), 2389.
13) M. Hillert and L.-I. Staffansson: *Acta Chem. Scand.*, **24** (1970), 3618.
14) N. Saunders and A. P. Miodownik: Calphad, Calculation of Phase Diagrams, A Comprehensive Guide, Pergamon, Oxford, UK, (1988), 91.
15) T. Miki and M. Hino: *ISIJ Int.*, **44** (2004), 1800.
16) T. Miki and M. Hino: *ISIJ Int.*, **45** (2005), 1848.
17) C. Wagner: Thermodynamics of Alloys, Addison-Wesley Press, Cambridge, MA, (1952), 47.
18) Y. Kang, M. Thunman, D. Sichen, T. Morohoshi, K. Mizukami and K. Morita: *ISIJ Int.*, **49** (2009), 1483.
19) M. K. Paek, J. M. Jang, Y. B. Kang and J. J. Pak: *Metall. Mater. Trans. B*, **46** (2015), 1826.
20) M. K. Paek, J. J. Pak and Y. B. Kang: *Metall. Mater. Trans. B*, **46** (2015), 2224.
21) W. Y. Cha, T. Nagasaka, T. Miki, Y. Sasaki and M. Hino: *ISIJ Int.*, **46** (2006), 996.
22) W. Y. Cha, T. Miki, Y. Sasaki and M. Hino: *ISIJ Int.*, **48** (2008), 729.
23) S. H. Seok, T. Miki and M. Hino: *ISIJ Int.*, **49** (2009), 804.
24) S. H. Seok, T. Miki and M. Hino: *ISIJ Int.*, **49** (2009), 1850.
25) M. Yonemoto, T. Miki and M. Hino: *ISIJ Int.*, **48** (2008), 755.
26) R. Yamamoto, H. Fukaya, N. Satoh, T. Miki and M. Hino: *ISIJ Int.*, **51** (2011), 895.
27) M. W. Chase, Jr. ed.: NIST-JANAF Thermochemical Tables, 4th ed., *J. Phys. Chem. Ref. Data*, American Institute of Physics, Melville, NY, (1998), 154.
28) I. Ansara, N. Dupin, H. L. Lukas and B. Sundman: *J. Alloy. Compd.*, **247** (1997), 20.
29) B.-J. Lee: *Calphad*, **17** (1993), 251.
30) N. Saunders: COST 507, Thermochemical Database for Light Metal Alloys, ed. by I. Ansara *et al.*, European Communities, Luxemburg, (1998), 34.
31) L. Zhang, J. Wang, Y. Du, R. Hu, P. Nash, X. G. Lu and C. Jiang: *Acta Mater.*, **57** (2009), 5324.
32) J. Miettinen: *Calphad*, **23** (1999), 249.
33) C. W. Bale, E. Bélisle, P. Chartrand, S. A. Decterov, G. Eriksson, K. Hack, I. H. Jung, Y. B. Kang, J. Melançon, A. D. Pelton, C. Robelin and S. Petersen: *Calphad*, **33** (2009), 295.